Research Article

Received: 21 August 2013 Revised: 29 November 2013 Accepted article published: 4 December 2013 Published online in Wiley Online Library: 2 January 2014

(wileyonlinelibrary.com) DOI 10.1002/jctb.4284

Photonic and quantum efficiencies for the homogeneous photo-Fenton degradation of herbicide 2,4-D using different iron complexes

Leandro O. Conte,[a] Pedro Querini,[b] Enrique D. Albizzati[c] and Orlando M. Alfano[a,b]*

Abstract

BACKGROUND: An experimental study of the homogeneous photo-Fenton degradation of herbicide 2,4-dichlorophenoxyacetic acid (2,4-D) is presented. Different sources of iron in water solution were studied: sulphate, oxalate and citrate complexes. The performances of these complexes were evaluated by means of two parameters: (i) the photonic efficiencies of degradation and mineralization; and (ii) the quantum efficiencies of degradation and mineralization. Moreover, in order to quantify the consumption of the oxidizing agent, two parameters were also defined and evaluated: the 'initial specific consumption of the hydrogen peroxide' and the 'minimum hydrogen peroxide consumption for complete mineralization'.

RESULTS: For pH = 5 and $T = 35^{\circ}C$, the degradation photonic efficiency using ferric sulphate was 6 times lower than that obtained with the ferric citrate. On the contrary, at pH = 5, quantum efficiencies of mineralization close to 50% for citrate and oxalate complexes were attained. For pH = 5 and 25 or $35^{\circ}C$, the initial specific consumption of hydrogen peroxide for the ferric sulphate was 5 times higher than those of the remaining complexes. However, considering all the operating conditions, the minimum hydrogen peroxide consumption for complete mineralization using the oxalate complex was always lower than or at most similar to those observed in the other two complexes.

CONCLUSION: Using different sources of iron, the influence of pH and temperature on the pollutant degradation and mineralization process was determined. For pH = 5 and both temperatures, the ferric sulphate system required more than twice the time to achieve complete degradation of the herbicide. Moreover, mineralization only reached 55% after 180 min operation.

Supporting information may be found in the online version of this article.

Keywords: photo-Fenton; iron complexes; photonic efficiency; quantum efficiency; 2,4-D

INTRODUCTION

2,4-dichlorophenoxyacetic acid (2,4-D) is one of the most frequently used systemic herbicides, mainly in the control of broadleaf weeds. Due to its low cost and high efficiency, it has been used steadily for decades. However, this herbicide presents a high level of toxicity and relatively high solubility in water, which facilitates its migration to natural courses where it may last for several weeks due to its long mean life time. Its use has generated considerable controversy about the benefits and the environmental damage it causes.

In recent years, advanced oxidation processes (AOPs) and sulphate radical advanced oxidation processes (SR-AOPs) have been considered viable alternatives for the treatment of wastewaters containing toxic compounds that cannot be removed by means of conventional purification systems.[1] In particular, the photo-Fenton process is one of the AOPs that has been successfully applied for the treatment of liquid wastes containing residues of agrochemicals.[2–5] This reaction produces highly oxidizing species that are generated from the combination of iron salts and HP (hydrogen peroxide), under natural or artificial

* *Correspondence to: O. M. Alfano, Instituto de Desarrollo Tecnológico para la Industria Química (INTEC), Consejo Nacional de Investigaciones Científicas y Técnicas (CONICET) and Universidad Nacional del Litoral (UNL), Ruta Nacional N° 168, 3000 Santa Fe, Argentina. E-mail: alfano@intec.unl.edu.ar*

a *Instituto de Desarrollo Tecnológico para la Industria Química (INTEC), Consejo Nacional de Investigaciones Científicas y Técnicas (CONICET) and Universidad Nacional del Litoral (UNL), Ruta Nacional N° 168, 3000, Santa Fe, Argentina*

b *Facultad de Ingeniería y Ciencias Hídricas, UNL, Ruta Nacional N° 168 - km 472,4, 3000, Santa Fe, Argentina*

c *Facultad de Ingeniería Química, UNL, Santiago del Estero 2654, 3000, Santa Fe, Argentina*

irradiation.[6,7] Recently, synergistic effects of the photo-Fenton process combined with other AOPs have also been reported.[8–10]

The use of ferric/ferrous iron salts (e.g. ferric sulphate) in homogeneous photo-Fenton reactions is limited by a narrow pH range for application. The optimum operating pH is close to 3; this value maximizes the concentration of mono and di-hydroxylated aqueous complexes of Fe(III), which absorb UV radiation more efficiently in comparison with non-hydroxylated Fe(III) complexes.[3] Furthermore, at pHs higher than 3 Fe(III) precipitates as hydroxides thereby decreasing the concentration of catalyst for the homogeneous reaction. However, various organic ligands especially polydentate can strongly complex the Fe(III). These compounds typically have higher molar radiation absorption coefficients (UV/visible region) when they are compared with the aqueous complexes.[6] It has been shown that complexes of ferric oxalate[11,12] and ferric citrate[13] have a broader absorption spectrum in the UV/visible region, so that they could be used in the solar photo-Fenton process.

Several contributions have been reported in the literature using these types of Fe(III) complexes to study the photo-Fenton degradation of pesticides,[13–17] non-biodegradable dyes,[18] and emerging contaminants.[19,20]

The aim of this work is to study the homogeneous photo-Fenton degradation of herbicide 2,4-D in water, employing different types of iron source. The behaviour of sulphate, oxalate and ferric citrate complexes, under different operating conditions of pH (3 and 5) and reaction temperature (25 and 35 °C) were investigated. To do this, the performances of these complexes were evaluated by means of two parameters: (i) the photonic efficiencies of degradation and mineralization; and (ii) the quantum efficiencies of degradation and mineralization. To compute the photon absorption rate in the homogeneous photoreactor, the volumetric absorption coefficients of the three complexes were evaluated experimentally by UV-visible spectrophotometry for both pHs and temperatures. In order to quantify the consumption of the oxidizing agent, two parameters were also defined and evaluated: the 'initial specific consumption of the hydrogen peroxide' and the 'minimum hydrogen peroxide consumption for complete mineralization'.

THEORETICAL

In order to quantify and compare the photo-Fenton degradation of herbicide 2,4-D under different operating conditions, two degradation efficiencies were evaluated: the photonic efficiency ($\eta_{2,4-D,pho}$) and the quantum efficiency ($\eta_{2,4-D,qua}$).

$$\eta_{2,4-D,pho} = \frac{amount\ of\ 2,4-D\ converted}{amount\ of\ \ photons\ arriving\ at\ the\ reactor\ window} = R^0_{2,4-D}\frac{V_R}{q_W A_W} \quad (1)$$

$$\eta_{2,4-D,qua} = \frac{amount\ of\ 2,4-D\ converted}{amount\ of\ \ photons\ absorbed\ by\ the\ reagent\ solution} = R^0_{2,4-D}\frac{V_R}{V_R\,\langle e^a(x,t)\rangle_{V_R}} \quad (2)$$

where q_W is the local radiation flux averaged over the reactor window (A_W) and $\langle e^a(x,t)\rangle_{V_R}$ the local volumetric rate of photon absorption (LVRPA) integrated over useful wavelengths ($\lambda min = 320$ nm and $\lambda max = 410$ nm) and averaged over the reactor volume (V_R). In Equations 1 and 2, $R^0_{2,4-D} = \left.\frac{dC_{2,4-D}}{dt}\right|_{t=0}$ represents the instantaneous rate of 2,4-D decomposition evaluated at $t = 0$.

Besides, with the goal of quantifying the complete mineralization of 2,4-D, the photonic ($\eta_{TOC,pho}$) and quantum ($\eta_{TOC,qua}$) mineralization efficiencies were determined:[21,22]

$$\eta_{TOC,pho} = \frac{amount\ of\ TOC\ converted}{amount\ of\ \ photons\ arriving\ at\ the\ reactor\ window} = R^0_{TOC}\frac{V_R}{q_W A_W} \quad (3)$$

$$\eta_{TOC,abs} = \frac{amount\ of\ TOC\ converted}{amount\ of\ \ photons\ absorbed\ by\ the\ reagent\ solution} = R^0_{TOC}\frac{V_R}{V_R\,\langle e^a(x,t)\rangle_{V_R}} \quad (4)$$

In Equations 3 and 4, $R^0_{TOC} = \left.\frac{dC_{TOC}}{dt}\right|_{t=0}$ represents the instantaneous rate of total organic carbon (TOC) degradation (or 2,4-D mineralization) evaluated at $t = 0$.

The photonic efficiencies relate the amount of moles of pollutant (or TOC) converted with the quantity of photons arriving at the reactor window, over a defined range of wavelengths. In real situations, not all the incident photons are absorbed by the reacting solution. On the other hand, the quantum efficiencies are the ratio between the moles of pollutant (or TOC) degraded and the quantity of photons absorbed by the reagent, over a defined spectral range. These efficiency parameters are used to make objective comparisons of the pollutant degradation or mineralization extent reached under different operating conditions. Additionally, the knowledge of these efficiencies is an indicative measure of the energy performance attained with the process.

EXPERIMENTAL

Materials

2,4-diclorophenoxiacetic acid (Merck, 98%) was employed as the model pollutant. The experiments were performed employing iron sulphate (Carlo Erba, RPE), analytic-grade ferric citrate monohydrate (Anedra, 21%) and reagent-grade HP (Carlo Erba, ACS, 30%). The potassium ferrioxalate was prepared in the laboratory according to the methodology reported by Murov *et al.*[23] Concentrated sulphuric acid (95–98% pro-analysis, Ciccarelli p.a.) and NaOH (reagent-grade, Mallinckrodt) were employed for pH adjustment.

Setup and procedure

The apparatus employed was an isothermal, well-stirred tank photoreactor, irradiated from the bottom with a mercury-vapour fluorescent lamp (Philips TL 40 W/09 N) placed at the focal axis of a cylindrical reflector of parabolic cross-section. The tank was equipped with a thermometer, a liquid sampling valve, a variable-speed stirrer, and a shutter to isolate the reactor bottom from the emitting system (Fig. 1). The experimental device was connected to a thermostatic bath to ensure isothermal conditions

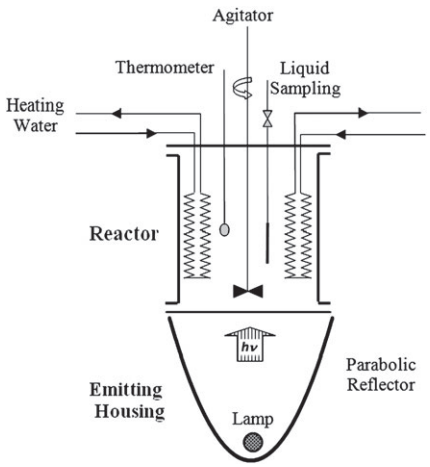

Reactor dimensions	Value	Units
Total liquid volume	3.00×10^{-3}	m^3
Diameter	1.42×10^{-1}	m
Length (L_R)	1.89×10^{-1}	m
Window area (A_w)	1.58×10^{-2}	m^2

Figure 1. Schematic representation of the stirred tank laboratory photoreactor.

during the experimental runs. More details on this laboratory tank photoreactor can be found elsewhere.[24]

Experimental runs began when solutions of ferric complex and 2,4-D were added to the reactor with distilled water at ambient temperature; concentrated sulphuric acid or sodium hydroxide was used to adjust the pH. Then, the temperature of the thermostatic bath was fixed at the specified working condition, the HP solution added to the reactor, and the first sample withdrawn, defining the reaction time equal to zero. Once the specified operating conditions were reached, the lamp shutter was removed to start the photo-Fenton run. During the experimental run, the reaction temperature was kept constant and liquid samples were taken at different times.

Analysis

2,4-D concentration was analyzed by HPLC using a Waters chromatograph equipped with a LC-18 Supelcosil reversed phase column (Supelco). The eluent flow rate was 1 $cm^3\ min^{-1}$; it was a binary mixture of distilled water (containing 1% v/v acetic acid) and acetonitrile in proportion 50:50. Detection was done at 236 and 280 nm. HP was analyzed with a modified iodimetric technique and ferrous ions with absorbance measurements of the Fe(II)-phenantroline complex at 510 nm. The mineralization of the herbicide was evaluated by means of TOC measurements employing a Shimadzu TOC-5000A analyzer.

For all tests, the pollutant concentration was 30 mg L^{-1}. The HP to 2,4-D initial molar ratio (R) was 28.5. Accordingly, the initial concentration of HP was 131.5 mg L^{-1} (3.87 mmol L^{-1}).

Under similar operating conditions, the repeatability of central experimental runs was verified. The maximum errors of 2,4-D, HP, TOC (2–10 mg L^{-1}) and TOC (10–40 mg L^{-1}) concentrations were 0.115 mg L^{-1}, 4.406 mg L^{-1}, 0.395 mg L^{-1} and 1.145 mg L^{-1}, respectively.

RADIATION MODEL

For the evaluation of the denominator of the photonic degradation efficiency (Equation 1) and the photonic mineralization efficiency (Equation 3), the local radiation flux averaged over the reactor window was measured by potassium ferrioxalate actinometry.[23] From the experimental results, the following value was determined: $q_W = 1.67 \times 10^{-8}$ Einstein $cm^{-2}\ s^{-1}$.

Similarly, to evaluate the denominator of the quantum degradation efficiency (Equation 2) and the quantum mineralization efficiency (Equation 4), it is necessary to know the LVRPA averaged over the reactor volume.

According to the assumptions proposed by Alfano *et al.*[25] for a similar laboratory photoreactor, a one-dimensional radiation field model has been used in this work to calculate the monochromatic LVRPA as a function of the spatial coordinate x. Thus,

$$e^a_\lambda(x,t) = \kappa_\lambda(t)\, q_W f_\lambda \exp\left(-\kappa_{T,\lambda}(t)\, x\right) \tag{5}$$

In Equation 5, f_λ is the normalized spectral distribution of the lamp output power provided by the supplier, κ_λ the volumetric absorption coefficient of the reacting species, and $\kappa_{T,\lambda}$ the total volumetric absorption coefficient of the medium.

Because the lamp output power and the optical properties of the reactants are functions of wavelength, an integration over all the useful wavelengths must be performed to compute $e^a(x,t)$. Thus, the polychromatic LVRPA is calculated from the following expression

$$e^a(x,t) = \int_{\lambda_{min}}^{\lambda_{max}} e^a_\lambda(x,t)\, d\lambda \cong \sum_\lambda e^a_\lambda(x,t) \tag{6}$$

Finally, the average value of $e^a(x,t)$ in the reactor volume, considering that the cross-section of the reactor is constant, can be computed as

$$\left\langle e^a(x,t)\right\rangle_{V_R} = \frac{1}{L_R} q_W \sum_\lambda f_\lambda \left[1 - \exp\left(-\kappa_{T,\lambda}(t)\, L_R\right)\right] \tag{7}$$

where L_R is the reactor depth.

RESULTS AND DISCUSSION

The reaction rate and the photonic and quantum efficiencies of the photo-Fenton degradation of 2,4-D, as well as the TOC degradation and the photonic and quantum efficiencies of the mineralization process, were studied considering the effect of three working variables: (i) iron complex (sulphate, citrate and oxalate); (ii) reaction temperature (25 and 35 °C); and (iii) initial pH

Table 1. Operating conditions and volumetric absorption coefficients at 350 nm

	Runs	pH	T (°C)	$\kappa_{T,350}$ (cm^{-1})
Ferric sulphate	S:3–25	3	25	0.074
	S:3–35	3	35	0.082
	S:5–25	5	25	< 0.005
	S:5–35	5	35	< 0.005
Ferric oxalate	O:3–25	3	25	0.117
	O:3–35	3	35	0.113
	O:5–25	5	25	0.157
	O:5–35	5	35	0.149
Ferric citrate	C:3–25	3	25	0.083
	C:3–35	3	35	0.086
	C:5–25	5	25	0.180
	C:5–35	5	35	0.178

of the reacting solution (3 and 5). It is worth noting that this pH range covers the natural values that can be usually found for 2,4-D aqueous solution concentrations up to 100 mg L^{-1}. Table 1 presents a summary of the operating conditions of the experimental runs.

Volumetric absorption coefficients

Radiation absorption is dependent on the iron species present in the medium for each complex analyzed; this speciation is determined by the source and concentration of iron, pH and temperature of operation. Therefore, for all the operating conditions employed in the experiments, the volumetric absorption coefficients were determined experimentally by UV-visible spectrophotometry. The iron concentration was 3 mgL^{-1} (5.37×10^{-5} mol L^{-1}). All samples analyzed in the spectrophotometer were previously filtered through nylon filters of 0.22 µm. Values of $\kappa_{T,\lambda}$ for the three iron complexes and over all the useful wavelengths are presented in Tables S1 – S4 (Supporting Information). For comparative purposes, Table 1 shows only the corresponding values of $\kappa_{T,\lambda}$ at a wavelength of 350 nm, the emission peak of the UV lamp.

Note that the ferric sulphate system at pH = 5, and T = 25 or 35 °C (Runs S:5–25 or S:5–35) had no radiation absorption in the range of wavelength analyzed ($\kappa_{T,350} < 0.005$). For these operating conditions, the iron was completely in colloidal form (hydroxides) which was retained when the sample was filtered. However, for all other complexes and working conditions there were no differences in the spectra obtained between filtered and unfiltered samples. Thus, it is important to emphasize the 'stabilization of iron' provided by the oxalate and citrate complexes, even under conditions of pH = 5. For the typical operating conditions of the photo-Fenton reaction (pH = 3), the ferric oxalate presented the greatest volumetric absorption coefficients; for example, at T = 25 °C, $\kappa_{T,350}$ was 58% higher than the corresponding value of the ferric sulphate. However, for pH = 5 the ferric citrate showed the highest values of volumetric absorption coefficient.

2,4-D and TOC experimental results

Figure 2 presents the time evolution of 2,4-D concentration under different working variables (runs S:3–25 to C:5–35). For pH = 3 and T = 25 °C, a similar behaviour was obtained for the three ferric complexes (Fig. 2(a)). The beneficial effect of increasing the reaction temperature can be observed.[26–28] A temperature increase of 10 °C produced a higher degradation rate, reaching complete destruction of 2,4-D in only 20 min of reaction.

For conditions of pH = 5 (Fig. 2(b)) a much longer reaction time (180 min) was necessary to reach almost complete conversion of 2,4-D at the highest temperature of 35 °C. On the contrary, for the oxalate and citrate complexes at T = 35 °C, it was possible to achieve the complete conversion of the herbicide after only 45 min.

The effect of each ferric complex on the time evolution of the TOC was also analyzed under the different operating conditions (Fig. 3). It is interesting to note that the depletion of TOC shown in this figure includes the destruction of the pollutant (2,4-D and reaction intermediates) plus the removal of the organic fraction of the ferric complex. For example, for the iron concentration employed in this work (3 mg L^{-1}), the contributions to TOC produced by the ferric oxalate and citrate complexes are 3.87 and 3.85 mg L^{-1}, respectively.

For the experimental conditions pH = 3 and T = 35 °C (Fig. 3(a)), the mineralization of the sample was achieved in a considerably shorter time for oxalate and citrate complexes (t = 45 min) than for the sulphate system (t = 60 min). Moreover, for pH = 5 and T = 25 or 35 °C (Fig. 3(b)), total mineralization of the sample for the ferric sulphate system was not achieved; only 40% TOC conversion was reached at T = 35 °C. In contrast, for the ferric oxalate system under similar operating conditions, TOC conversion was nearly 100% in just 90 min of reaction time.

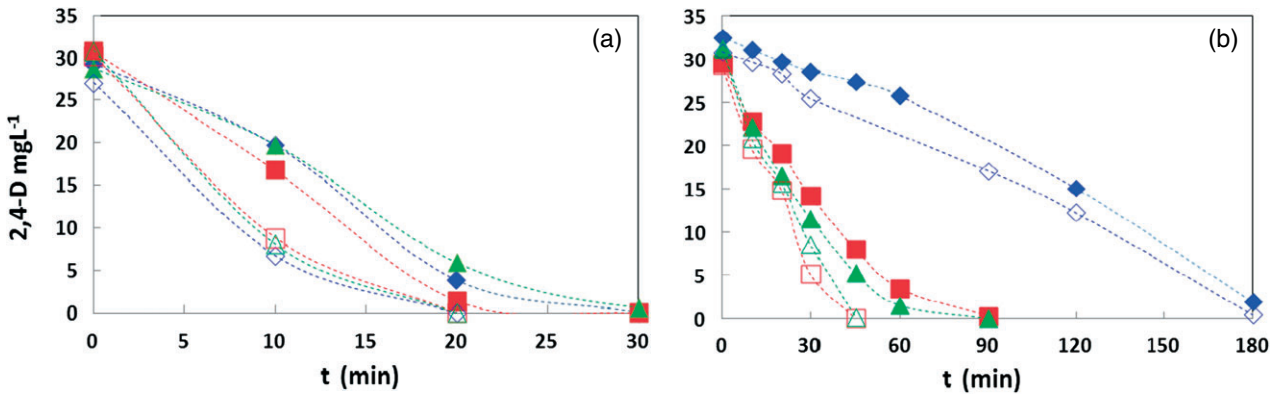

Figure 2. Time evolution of 2,4-D concentration. (a) pH = 3. (b) pH = 5. Keys: T = 25°C (closed symbols) and T = 35°C (open symbols). Ferric Sulphate (◆), Ferric Oxalate (■), and Ferric Citrate (▲).

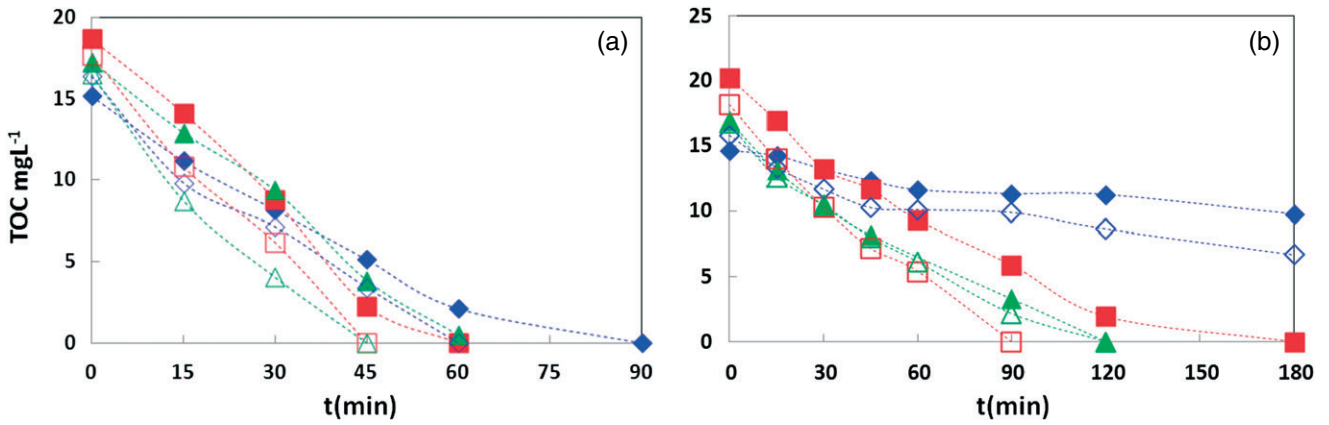

Figure 3. Time evolution of TOC concentration. (a) pH = 3. (b) pH = 5. Keys: T = 25 °C (closed symbols) and T = 35 °C (open symbols). Ferric Sulphate (◆), Ferric Oxalate (■), and Ferric Citrate (▲).

Photonic and quantum efficiencies

For the operating conditions summarized in Table 1, the LVRPA averaged over the reactor volume was computed (Table 2, second column). Working at pH = 3, the ferric oxalate showed the highest value of $\langle e^a(x,t)\rangle_{V_R}$. At $T = 25\,^{\circ}C$, the corresponding value of $\langle e^a(x,t)\rangle_{V_R}$ was 25% higher than that obtained for the ferric sulphate system (runs O:3–25 vs. S:3–25). However, for pH = 5, ferric citrate had the highest value of $\langle e^a(x,t)\rangle_{V_R}$. These results are consistent with the differences observed in the values of the volumetric absorption coefficients (Table 1 and Supporting Information).

Considering these results for the LVRPA averaged over the reactor volume and the temporal evolution of 2,4-D and TOC previously reported, the degradation and mineralization efficiencies were computed. A summary of the results is presented in Table 2.

For the three complexes analyzed the highest rates of herbicide degradation ($R^0_{2,4-D}$) and mineralization (R^0_{TOC}) were found at the working conditions pH = 3 and $T = 35\,^{\circ}C$ (runs S:3–35, O:3–35 and C:3–35), the maximum degradation rate being the one obtained with ferric citrate complex (2.273 mg L^{-1} 2,4-D min^{-1} and 0.485 mg L^{-1} TOC min^{-1}). On the other hand, for the operating conditions pH = 5 and $T = 25$ or $35\,^{\circ}C$, the ferric sulphate system presented the lowest degradation rates (runs S:5–25 and S:5–35). For example, at $T = 25\,^{\circ}C$, the R^0_{TOC} of this system was 8 times lower than that obtained using ferric citrate (runs S:5–25 and C:5–25). Besides, $R^0_{2,4-D}$ obtained with the ferric sulphate was only 22% compared with that observed for the ferric oxalate complex (runs S:5–25 and O:5–25).

Considering the results of photonic and quantum efficiencies for the operating conditions pH = 3 and $T = 25\,^{\circ}C$, one can observe that similar values of $\eta_{2,4-D,pho}$ and $\eta_{2,4-D,qua}$ were reached for the three complexes (runs S:3–25, O:3–25 and C:3–25); among them, the oxalate complex presented the better performance. After raising the operating temperature from 25 to $35\,^{\circ}C$, over 50% increases in the values of $\eta_{2,4-D,pho}$ and $\eta_{2,4-D,qua}$ were observed. For instance, these increments were close to 150% for the ferric citrate complex (runs C:3–25 and C:3–35). However, when increasing the pH from 3 to 5, at $T = 25$ or $35\,^{\circ}C$, these degradation efficiencies decreased for all complexes, still being important for the oxalate and citrate complexes and almost zero for the ferric sulphate system. Notice that under the working conditions pH = 5 and $T = 35\,^{\circ}C$, the $\eta_{2,4-D,pho}$ for the ferric sulphate system was 6 times lower than that obtained with ferric citrate (see runs S:5–35 and C:5–35).

Table 2. Effect of different ferric complexes and reaction temperatures on the 2,4-D and TOC photonic and quantum efficiencies

				Degradation efficiencies		Mineralization efficiencies	
Runs	$\langle e^a(x,t)\rangle_{V_R} \times 10^{10}$ (Einstein cm^{-3} s^{-1})	$R^0_{2,4-D}$ (mg L^{-1} 2,4-D min^{-1})	R^0_{TOC} (mg L^{-1} TOC min^{-1})	$\eta_{2,4-D,pho}$	$\eta_{2,4-D,qua}$	$\eta_{TOC,pho}$	$\eta_{TOC,qua}$
S:3–25	5.822	0.951	0.272	0.081	0.123	0.425	0.644
O:3–25	7.304	1.402	0.306	0.120	0.145	0.473	0.571
C:3–25	6.711	0.904	0.294	0.077	0.101	0.458	0.603
S:3–35	6.051	2.032	0.424	0.174	0.253	0.662	0.964
O:3–35	7.151	2.214	0.461	0.189	0.233	0.725	0.893
C:3–35	6.773	2.273	0.485	0.195	0.253	0.756	0.985
S:5–25	---	0.145	0.032	0.012	---	0.047	---
O:5–25	7.993	0.663	0.224	0.056	0.062	0.347	0.382
C:5–25	8.322	0.892	0.258	0.076	0.081	0.394	0.417
S:5–35	---	0.176	0.105	0.015	---	0.158	---
O:5–35	7.876	0.962	0.283	0.083	0.092	0.441	0.494
C:5–35	8.296	1.056	0.283	0.090	0.095	0.441	0.469

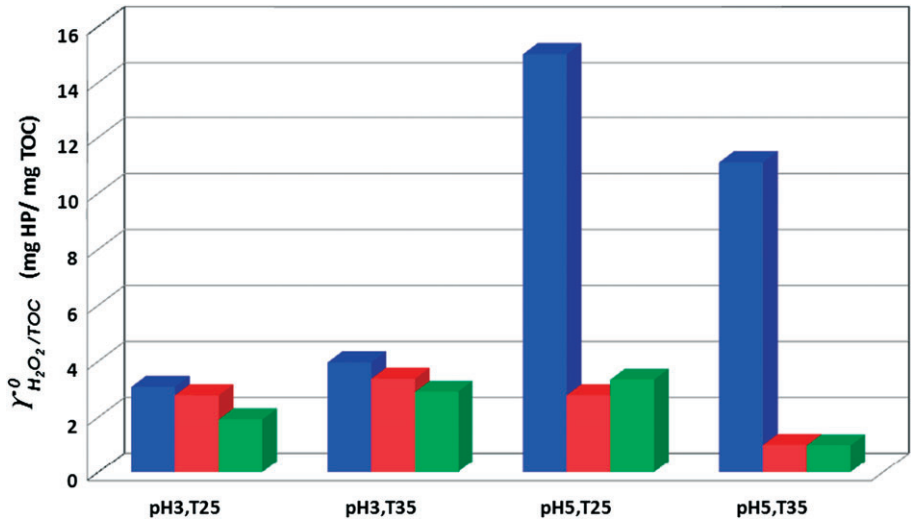

Figure 4. Initial Specific Consumption of the Oxidizing Agent ($\Upsilon^{0}_{H_2O_2/TOC}$). Ferric Sulphate (▦), Ferric Oxalate (▩) and Ferric Citrate (■).

Regarding the mineralization efficiencies for all iron complexes, it can be noted that they were all above 40% for pH = 3 and $T = 25\ ^{\circ}C$, reaching a maximum value of $\eta_{TOC,pho}$ equal to 64.4% for the ferric sulphate system. Nevertheless, by increasing the operating pH from 3 to 5, these mineralization efficiencies were decreased for all the complexes, still being high and close to 40% for the oxalate and citrate systems (runs O:5–25 and C:5–25) and almost zero for the ferric sulphate ($\eta_{TOC,pho} = 0.047$ for run S:5–25). Again, an important effect of the reaction temperature over the process was observed. Note that, even at pH = 5, values of $\eta_{TOC,qua}$ close to 50% for citrate and ferric oxalate complexes were achieved (runs O:5–35 and C:5–35).

In general, lower degradation and mineralization efficiencies were obtained in the runs S:5–25 and S:5–35 for the ferric sulphate system. Under these experimental conditions (pH = 5), the iron was found completely in colloidal form.

Few contributions have been reported in the literature relative to the evaluation of photo-Fenton photonic efficiencies. Sioi *et al.*[29] reported an initial $\eta_{TOC,pho} = 0.4526$ for synthetic Harris' Hematoxylin solution mineralization, under the following operating conditions: pH = 3.1, Hematien = 50 mg L^{-1}, Fe^{+3} = 56 mg L^{-1}, HP = 1 g L^{-1} and visible light illumination. Kitsiou *et al.*[30] published an initial $\eta_{imidacloprid,pho} = 0.0025$ for pH = 3.2, imidacloprid = 20 mg L^{-1}, Fe^{+3} = 7 mg L^{-1}, HP = 200 mg L^{-1} and oxalate ions = 33 mg L^{-1}; under these operating conditions an initial $\eta_{TOC,pho} = 0.3641$ was reached. For the degradation of nonylphenol ethoxylate-9 (NPE-9), De la Fuente *et al.*[31] reported an initial $\eta_{NPE-9,pho} = 0.0778$, for pH = 2.8, NPE-9 = 0.48 mmol L^{-1}, Fe^{+2} = 0.24 mmol L^{-1} and HP = 0.96 mmol L^{-1}.

Oxidizing agent consumption

In the photo-Fenton degradation process of organic compounds, it is important to evaluate the consumption of HP during the treatment. Therefore, a useful parameter to evaluate HP consumption for this process is the 'initial specific consumption of

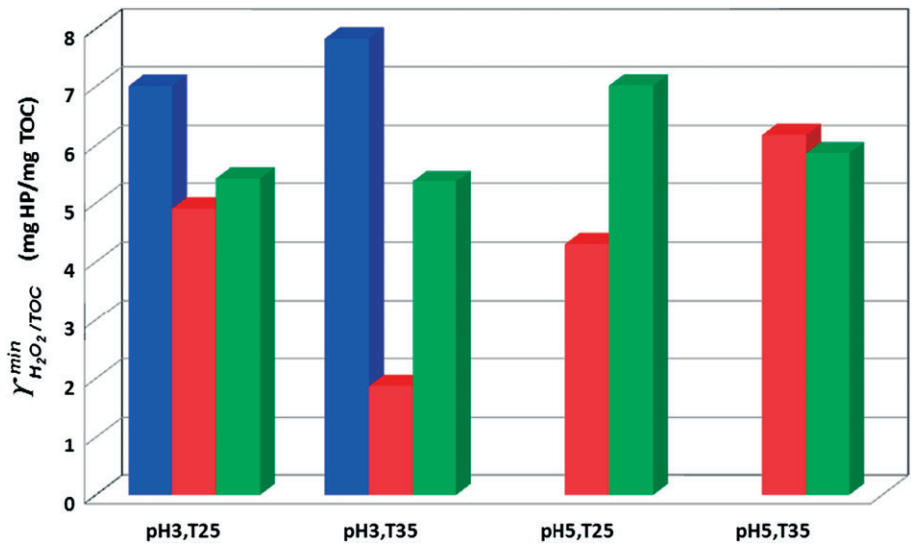

Figure 5. Minimum Hydrogen Peroxide Consumption needed to achieve the Mineralization of the sample ($\Upsilon^{min}_{H_2O_2/TOC}$). Ferric Sulphate (▦), Ferric Oxalate (▩) and Ferric Citrate (■).

the oxidizing agent' ($\Upsilon^0_{H_2O_2/TOC}$), defined as

$$\Upsilon^0_{H_2O_2/TOC} = \frac{R^0_{H_2O_2}}{R^0_{TOC}} \quad (8)$$

In Equation (8) $R^0_{H_2O_2} = \left.\frac{dC_{H_2O_2}}{dt}\right|_{t=0}$ and $R^0_{TOC} = \left.\frac{dC_{TOC}}{dt}\right|_{t=0}$ represent the initial rate of HP consumption and the initial rate of herbicide mineralization, respectively.

A multiple bar chart can be employed to show the effects of pH and reaction temperature on the computed values of $\Upsilon^0_{H_2O_2/TOC}$ for all experimental runs (Fig. 4). Under the operating conditions pH = 5 and both reaction temperatures (25 and 35 °C), $\Upsilon^0_{H_2O_2/TOC}$ is considerably higher for the ferric sulphate system. In contrast, low values of $\Upsilon^0_{H_2O_2/TOC}$ are found for the oxalate and citrate complexes.

Very few studies have been identified with an assessment of the specific consumptions of the oxidant agent. For the heterogeneous photo-Fenton degradation of acetic acid, Sannino *et al.*[32] reported a HP specific consumption of 5.5 mol HP per mol C obtained after 4 h of reaction and the following operating conditions: acetic acid = 0.021 mol L^{-1} and HP = 0.083 mol L^{-1}.

Note that when working with ferric sulphate at pH = 5, HP can be additionally decomposed to water and oxygen via a non-radical pathway by iron oxides generated during the iron compounds precipitation at pH higher than 3.[33,34]

Another practical parameter to evaluate HP consumption for the photo-Fenton process is the 'minimum hydrogen peroxide consumption needed to achieve mineralization' ($\Upsilon^{min}_{H_2O_2/TOC}$). This parameter can be defined as

$$\Upsilon^{min}_{H_2O_2/TOC} = \frac{C^0_{H_2O_2} - C^{min}_{H_2O_2}}{C^0_{TOC}} \quad (9)$$

In Equation 9, $C^{min}_{H_2O_2}$ represents the concentration of the oxidizing agent remaining in the system when the total destruction of the organic carbon ($C_{TOC} = 0$) is achieved, and $C^0_{H_2O_2}$ and C^0_{TOC} are the initial concentrations of HP and TOC, respectively.

Figure 5 shows the effects of pH and reaction temperature on $\Upsilon^{min}_{H_2O_2/TOC}$, for each of the experimental runs. First, under experimental conditions pH = 5, mineralization of the sample was not achieved for the ferric sulphate system. At pH = 3 and T = 35 °C, and pH = 5 and T = 25 °C, lower oxidizing agent consumption was observed for the ferric oxalate complex. Taking into account all the operating conditions tested in the present work, the $\Upsilon^{min}_{H_2O_2/TOC}$ obtained with the oxalate complex was always less than or similar to the corresponding values observed for the other two complexes.

Finally, Fig. 5 shows that the minimum oxidizing agent consumption obtained with the oxalate complex is even lower than that observed working under the conventional operating conditions with ferric sulphate at pH = 3 and T = 25 °C.

CONCLUSIONS

In the range of wavelengths tested, we verified that under pH = 5 the radiation absorption of the aqueous solution of ferric sulphate was almost negligible. In contrast, under similar pH and T = 25 and 35 °C, the volumetric absorption coefficients at 350 nm were 0.157 and 0.148 cm^{-1} for the ferric oxalate complex and 0.179 and 0.178 cm^{-1} for the ferric citrate, respectively. Thus, it is important to emphasize the stabilization of iron provided by the oxalate and citrate complexes, even under conditions pH = 5.

For oxalate and citrate ferric complexes at pH = 5 and T = 25 °C, complete destruction of the herbicide after 90 min of reaction was achieved. Moreover, for the ferric citrate system and similar operating conditions, the mineralization of the sample was achieved after only 120 min.

For the three complexes analyzed, higher degradation and mineralization rates were measured for conditions pH = 3 and T = 35 °C, the maximum rates for the ferric citrate system being 2.273 mg L^{-1} 2,4-D min^{-1} and 0.485 mg L^{-1} TOC min^{-1}, respectively. In contrast, the lowest degradation and mineralization rates were obtained for the ferric sulphate system under pH = 5 and T = 25 or 35 °C. For T = 25 °C, the mineralization rate for the ferric sulphate system was 8 times lower than that obtained using ferric citrate.

Under the conventional operating conditions pH = 3 and T = 25 °C, similar 2,4-D photonic and quantum efficiencies were reached for the three complexes, with a better performance for the ferric oxalate. However, an increase higher than 50% in the values of the pollutant photonic and quantum efficiency was observed after raising the reaction temperature from 25 to 35 °C. On the other hand, when increasing the operating pH from 3 to 5, the mineralization efficiencies decreased for all complexes, still being high and close to 40% for the oxalate and citrate systems and almost zero for the ferric sulphate.

For pH = 5 and both reaction temperatures, the initial specific consumption of the hydrogen peroxide for the ferric sulphate system was 5 times higher than that of the remaining complexes. However, for pH = 3 this consumption is similar for the three systems analyzed and both reaction temperatures. Also, considering all the operating conditions tested in the present work, the minimum hydrogen peroxide consumption for complete mineralization achieved with the oxalate complex was always lower than or at most similar to the values observed for the other two complexes.

ACKNOWLEDGEMENTS

The authors are grateful to Universidad Nacional del Litoral (UNL), Consejo Nacional de Investigaciones Científicas y Técnicas (CONICET), and Agencia Nacional de Promoción Científica y Tecnológica (ANPCyT) for financial support. We also thank Antonio C. Negro for his valuable help during the experimental work.

Supporting Information

Supporting information may be found in the online version of this article.

REFERENCES

1 Zou J, Ma J, Chen L, Li X, Guan Y, Xie P and Pan C, Rapid acceleration of ferrous iron/peroxymonosulfate oxidation of organic pollutants by promoting Fe(III)/Fe(II) cycle with hydroxylamine. *Environ Sci Technol* **47**:11685–11691 (2013).
2 Al Momani FA, Shawaqfeh AT and Shawaqfeh MS, Solar wastewater treatment plant for aqueous solution of pesticide. *Sol Energy* **81**:1213–1218 (2007).
3 Malato S, Fernández-Ibañez P, Maldonado MI, Blanco J and Gernjak W, Decontamination and disinfection of water by solar photocatalysis: recent overview and trends. *Catal Today* **147**:1–59 (2009).
4 Zapata A, Oller I, Rizzo L, Hilgert S, Maldonado MI, Sánchez-Pérez JA and Malato S, Evaluation of operating parameters involved in solar photo-Fenton treatment of wastewater: interdependence of initial pollutant concentration, temperature and iron concentration. *Appl Catal B* **97**:292–298 (2010).

5 Ahmed B, Limem E, Abdel-Wahab A and Bensalah N, Photo-Fenton treatment of actual agro-industrial wastewaters. *Ind Eng Chem Res* **50**:6673–6680 (2011).
6 Pignatello JJ, Oliveros E and MacKay A, Advanced oxidation processes for organic contaminant destruction based on the Fenton reaction and related chemistry. *Crit Rev Env Sci Technol* **36**:1–84 (2006).
7 Neyens E and Baeyens J, A review of classic Fenton's peroxidation as an advanced oxidation technique. *J Hazard Mater* **98**:33–50 (2003).
8 Chen O, Ji F, Liu T, Yan P, Guan W and Xu X, Synergistic effect of bifunctional Co–TiO2 catalyst on degradation of Rhodamine B: Fenton-photo hybrid process. *Chem Eng J* **229**:57–65 (2013).
9 Kim H, Lee J, Lee H and Lee C, Synergistic effects of TiO2 photocatalysis in combination with Fenton-like reactions on oxidation of organic compounds at circumneutral pH. *Appl Catal B* **115–116**:219–224 (2012).
10 ThanhThuy T, Feng H and Cai Q, Photocatalytic degradation of pentachlorophenol on ZnSe/TiO2 supported by photo-Fenton system. *Chem Eng J* **223**:379–387 (2013).
11 Safarzadeh-Amiri A, Bolton JM and Cater SR, Ferrioxalate-mediated photodegradation of organic pollutants in contaminated water. *Water Res* **31**:787–798 (1996).
12 Nogueira R, Silva M and Trovó A, Influence of the iron source on the solar photo-Fenton degradation of different classes of organic compounds. *Sol Energy* **79**:384–392 (2005).
13 Silva M, Trovó A and Nogueira R, Degradation of the herbicide tebuthiuron using solar photo-Fenton process and ferric citrate complex at circumneutral pH. *J Photochem Photobiol A* **191**:187–192 (2007).
14 Nogueira R, Trovó A and Modé D, Solar photodegradation of dichloroacetic acid and 2,4-dichlorophenol using an enhanced photo-Fenton process. *Chemosphere* **48**:385–391 (2002).
15 Lee Y, Jeong J, Lee C, Kim S and Yoon J, Influence of various reaction parameters on 2,4-D removal in photo/ferrioxalate/H_2O_2 process. *Chemosphere* **51**:901–912 (2003).
16 Katsumata H, Kaneco S, Susuki T, Ohta K and Yobiko Y, Photo-Fenton degradation of alachlor in the presence of citrate solution. *J Photochem Photobiol A* **180**:38–45 (2006).
17 Monteagudo J, Durán A, Aguirre M and San Martín I, Optimization of the mineralization of a mixture of phenolic pollutants under a ferrioxalate-induced solar photo-Fenton process. *J Hazard Mater* **185**:131–139 (2011).
18 Monteagudo J, Durán A, San Martín I and Aguirre M, Catalytic degradation of Orange II in a ferrioxalate-assisted photo-Fenton process using a combined UV-A/C solar pilot-plant system. *Appl Catal B* **95**:120–129 (2010).
19 Trovó A and Nogueira R, Diclofenac abatement using modified solar photo-Fenton process with ammonium iron(III) citrate. *J Braz Chem Soc* **22**:1033–1039 (2011).
20 Trovó A, Nogueira R, Agüera A, Fernandez-Alba A and Malato S, Paracetamol degradation intermediates and toxicity during photo-Fenton treatment using different iron species. *Water Res* **46**:5374–5380 (2012).
21 Satuf M, Brandi R, Cassano A and Alfano O, Quantum efficiencies of 4-chlorophenol photocatalytic degradation and mineralization in a well-mixed slurry reactor. *Ind Eng Chem Res* **46**:43–51 (2007).
22 Benzaquén TB, Isla MA and Alfano OM. Quantum efficiencies of the photo-Fenton degradation of atrazine in water. *Water Sci Technol* **66**:2209–2216 (2012).
23 Murov S, Carmichael I and Hug G, *Handbook of Photochemistry*, 2nd edn. Marcel Dekker, New York, 299–305 (1993).
24 Conte L, Farias J, Albizzati E and Alfano O, Photo-Fenton degradation of the herbicide 2,4-D in laboratory and solar pilot-plant reactors. *Ind Eng Chem Res* **51**:4181–4191 (2012).
25 Alfano O, Romero R and Cassano A, A cylindrical photoreactor irradiated from the bottom. *I. Radiation flux density generated by a tubular source and a parabolic reflector. Chem Eng Sci* **40**:2119–2127 (1985).
26 Sagawe G, Lehnard A, Lübber M and Bahnemann D. The insulated solar Fenton hybrid process: fundamental investigations. *Helv Chim Acta* **84**:3742–3759 (2001).
27 Gernjak W, Fuerhacker M, Fernández-Ibáñez P, Blanco J and Malato S, Solar photo-Fenton treatment-process parameters and process control. *Appl Catal B Environ* **64**:121–130 (2006).
28 Farias J, Albizzati E and Alfano O, Kinetic study of the photo-Fenton degradation of formic acid combined effects of temperature and iron concentration. *Catal Today* **144**:117–123 (2009).
29 Sioi M, Bolosis A, Kostopoulou E and Poulios I, Photocatalytic treatment of colored wastewater from medical laboratories: photocatalytic oxidation of hematoxylin. *J Photochem Photobiol A* **184**:18–25 (2006).
30 Kitsiou V, Filippidis N, Mantzavinos D and Poulios I, Heterogeneous and homogeneous photocatalytic degradation of the insecticide imidacloprid in aqueous solutions. *Appl Catal B* **86**:27–35 (2009).
31 De la Fuente L, Acosta T, Babay P, Curutchet G, Candal R and Litter MI, Degradation of Nonylphenol Ethoxylate-9 (NPE-9) by photochemical advanced oxidation technologies. *Ind Eng Chem Res* **49**:6909–6915 (2010).
32 Sannino D, Vaiano V, Ciambelli P and Isupova L, Mathematical modelling of the heterogeneous photo-Fenton oxidation of acetic acid on structured catalysts. *Chem Eng J* **224**:53–58 (2013).
33 Kwan WP and Voelker BM, Rates of hydroxyl radical generation and organic compound oxidation in mineral-catalyzed Fenton-like systems. *Environ Sci Technol* **37**:1150–1158 (2003).
34 Ortiz de la Plata GB, Alfano OM and Cassano AE, Decomposition of 2-chlorophenol employing goethite as Fenton catalyst. I. Proposal of a feasible, combined reaction scheme of heterogeneous and homogeneous reactions. *Appl Catal B* **95**:1–13 (2010).

